

# Calcium-sensitive potassium channelopathy in human epilepsy and paroxysmal movement disorder

Wei Du<sup>1,2,9</sup>, Jocelyn F Bautista<sup>3,4,9</sup>, Huanghe Yang<sup>5</sup>, Ana Diez-Sampedro<sup>6</sup>, Sun-Ah You<sup>1</sup>, Lejin Wang<sup>1</sup>, Prakash Kotagal<sup>3</sup>, Hans O Lüders<sup>3</sup>, Jingyi Shi<sup>5</sup>, Jianmin Cui<sup>5</sup>, George B Richerson<sup>6,7</sup> & Qing K Wang<sup>1,2,8</sup>

**The large conductance calcium-sensitive potassium (BK) channel is widely expressed in many organs and tissues, but its *in vivo* physiological functions have not been fully defined. Here we report a genetic locus associated with a human syndrome of coexistent generalized epilepsy and paroxysmal dyskinesia on chromosome 10q22 and show that a mutation of the  $\alpha$  subunit of the BK channel causes this syndrome. The mutant BK channel had a markedly greater macroscopic current. Single-channel recordings showed an increase in open-channel probability due to a three- to fivefold increase in  $\text{Ca}^{2+}$  sensitivity. We propose that enhancement of BK channels *in vivo* leads to increased excitability by inducing rapid repolarization of action potentials, resulting in generalized epilepsy and paroxysmal dyskinesia by allowing neurons to fire at a faster rate. These results identify a gene that is mutated in generalized epilepsy and paroxysmal dyskinesia and have implications for the pathogenesis of human epilepsy, the neurophysiology of paroxysmal movement disorders and the role of BK channels in neurological disease.**

Epilepsy is one of the most common and debilitating neurological disorders, affecting more than 40 million people worldwide<sup>1</sup>. Paroxysmal dyskinesias are another heterogeneous group of neurological disorders characterized by sudden, unpredictable, disabling attacks of involuntary movement often requiring life-long treatment. The coexistence of epilepsy and paroxysmal dyskinesia in the same individual or family is an increasingly recognized phenomenon<sup>2,3</sup>. The basic pathophysiology underlying the coexistence of epilepsy and paroxysmal dyskinesia is unknown, and no specific gene has been associated with it.

We studied a large family with coexistent generalized epilepsy and paroxysmal dyskinesia (GEPD; **Fig. 1**). Sixteen affected individuals developed epileptic seizures ( $n = 4$ ), paroxysmal nonkinesigenic

dyskinesia (PNKD;  $n = 7$ ) or both ( $n = 5$ ). The detailed clinical features of 13 affected individuals, who participated in subsequent genetic studies, are summarized in **Table 1**. An example of interictal electroencephalography (EEG) showing generalized spike-wave complexes is shown in **Figure 2**. Pedigree analysis suggested an autosomal dominant pattern of inheritance. We carried out a genome-wide linkage scan with 382 microsatellite markers that span human chromosomes 1–22 at an average interval of 10 cM. Markers *D10S580* and *D10S1730* on chromosome 10q22 showed significant linkage to GEPD with lod scores of 3.68 and 3.73, respectively. The chromosomal 10q22 region was the only region with a lod score  $\geq 2.0$ . Fine mapping and haplotype analysis using eight additional markers narrowed the disease-associated interval to a region of 8.4 cM flanked by markers *D10S1694* and *D10S201* (**Fig. 1**).

The 10q22 locus associated with GEPD contains 40 genes, including 33 known genes and 7 hypothetical genes. Owing to the importance of ion channels in epilepsy<sup>4</sup> and paroxysmal movement disorders such as episodic ataxia<sup>5</sup>, we hypothesized that mutations in genes encoding ion channels might cause GEPD and identified two genes encoding ion channels in 8.4-cM region: *VDAC2*, encoding voltage-dependent anion channel 2, and *KCNMA1*, encoding the pore-forming  $\alpha$  subunit of the BK (or Maxi-K) channel. We did not find any mutations in *VDAC2*. We identified a heterozygous A  $\rightarrow$  G transition in exon 10 of *KCNMA1* in the proband (IV-8) of the family (**Fig. 3a**). The A  $\rightarrow$  G transition results in the substitution of a negatively charged aspartic acid residue for a neutral glycine residue (D434G) in the regulator of conductance for  $\text{K}^+$  (RCK) domain (**Fig. 3a,b**). Amino acid residue Asp434 is conserved among *KCNMA1* channels from nematodes to humans (**Fig. 3c**). DNA sequence analysis detected the presence of mutation 1301A  $\rightarrow$  G in all 13 affected individuals that were genotyped and its absence in 5 unaffected individuals in the family (data not shown). This result was confirmed by restriction fragment length polymorphism analysis (**Supplementary Fig. 1** online). Furthermore,

<sup>1</sup>Center for Molecular Genetics, Department of Molecular Cardiology, Lerner Research Institute; Center for Cardiovascular Genetics, Department of Cardiovascular Medicine, The Cleveland Clinic Foundation; and Department of Molecular Medicine, Cleveland Clinic Lerner College of Medicine; Case Western Reserve University; Cleveland, Ohio 44195, USA. <sup>2</sup>Department of Biological, Geological, and Environmental Science, Cleveland State University, Cleveland, Ohio 44115, USA.

<sup>3</sup>Department of Neurology, The Cleveland Clinic Foundation, Cleveland, Ohio 44195, USA. <sup>4</sup>Department of Epidemiology and Biostatistics, Case Western Reserve University, Cleveland, Ohio 44106, USA. <sup>5</sup>Department of Biomedical Engineering, Washington University, St. Louis, Missouri 63130, USA. <sup>6</sup>Departments of Neurology and Cellular & Molecular Physiology, Yale University School of Medicine, New Haven, Connecticut 06520, USA. <sup>7</sup>VAMC, West Haven, Connecticut 06516, USA.

<sup>8</sup>Huazhong University of Science and Technology Human Genome Research Center, Wuhan, China. <sup>9</sup>These authors contributed equally to this work. Correspondence should be addressed to Q.K.W. ([wangq2@ccf.org](mailto:wangq2@ccf.org)).

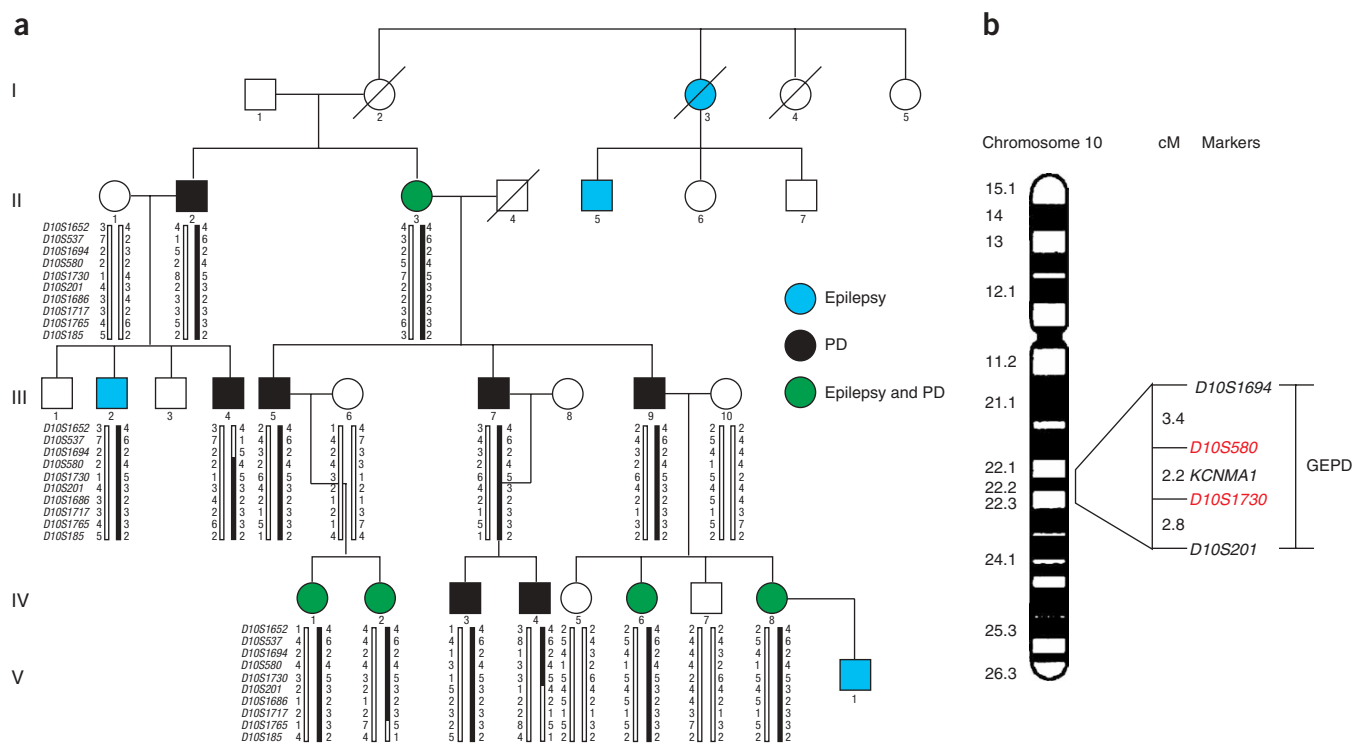


**Figure 1** Genetic linkage of GEPD to chromosome 10q22 in family QW1378. **(a)** Pedigree structure and genotypic analysis of the family affected with epilepsy (blue symbols), paroxysmal dyskinesia (PD; black symbols) or both (green symbols). Squares represent males; circles, females. Filled symbols denote affected individuals; open symbols, unaffected individuals. Symbols with slashes through them denote deceased individuals. The haplotype that cosegregated with the disease is indicated by a black vertical bar. **(b)** Ideogram of chromosome 10 showing Geimsa banding patterns, location of the GEPD-associated locus and location of *KCNMA1*.

the mutation was not detected in 500 unrelated healthy controls. These results suggest that the 1301A→G mutation of *KCNMA1* is responsible for GEPD in this large family.

The BK channel is activated by both membrane depolarization and a rise in cytosolic  $\text{Ca}^{2+}$  concentration. The pore-forming  $\alpha$  subunit contains seven transmembrane domains (S0–S6) at the N terminus and an extensive C terminus with four hydrophobic segments (S7–S10) and the  $\text{Ca}^{2+}$  bowl (Fig. 3b). Between S6 and S8 is the RCK

domain, which may contain binding sites for a variety of regulatory ligands, including  $\text{Ca}^{2+}$  and  $\text{Mg}^{2+}$  (Fig. 3b)<sup>6,7</sup>. As mutation D434G is located in the RCK domain, we hypothesized that the mutation could cause abnormal calcium affinity of the BK channel. We expressed wild-type and D434G mutant BK channels in both *Xenopus laevis* oocytes and mammalian Chinese hamster ovary (CHO) cells and recorded current-voltage relations. At a  $\text{Ca}^{2+}$  concentration of 2  $\mu\text{M}$ , there was more current induced at the same membrane potential in

**Table 1** Clinical features of 13 affected individuals in family QW1378 with GEPD

Individual	Age at onset of E	Seizure type	EEG	Age at onset of PD	Diagnosis
II-02	–	–	–	13–15 y	PD
II-03	6 y	Possible absence	Normal, as adult	6 y	E+PD
III-02	8–9 y	Possible absence	–	–	E
III-04	–	–	–	4–5 y	PD
III-05	–	–	Normal	7 y	PD
III-07	–	–	–	4–5 y	PD
III-09	–	–	–	3–4 y	PD
IV-01	<6 mo	Absence, rare GTC	SWC gen	<6 mo	E + PD
IV-02	3 y	Absence, rare GTC	SWC gen	<6 mo	E + PD
IV-03	–	–	Normal	4–5 y	PD
IV-04	–	–	Normal	4–5 y	PD
IV-06	5–6 y	Possible absence	Normal	5–6 y	E+PD
IV-08	2 y	Absence	SWC gen	2 y	E + PD

E, epilepsy; GTC, generalized tonic-clonic seizures; PD, paroxysmal dyskinesia; SWC gen, 3- to 4-Hz generalized spike-wave complexes typical of idiopathic generalized epilepsy. Individual V-1 was diagnosed with recurrent motor seizures in the first few weeks of life, which remitted without treatment, but EEG data was not available.

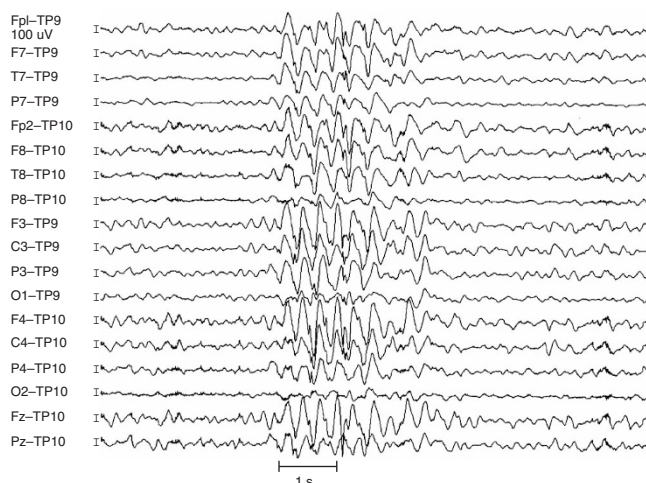


**Figure 2** Representative interictal EEG of an affected member of family QW1378 (individual IV-1) at 5 years of age. Ten-second EEG tracing showing interictal generalized spike-wave complexes (3–3.5 Hz) in an individual affected with both generalized epilepsy and paroxysmal dyskinesia.

oocytes expressing D434G channels than in oocytes expressing the wild-type channel, and the voltage dependence of steady-state activation (G-V relation) was shifted more than 57 mV toward more negative potentials by the D434G mutation, with little change in the slope of the curve (Fig. 4a,b). At a  $\text{Ca}^{2+}$  concentration of 0.1  $\mu\text{M}$ , the G-V relation was shifted  $\sim 26$  mV toward more negative potentials by the D434G mutation (Fig. 4b). These results indicate that the mutant BK channel has an increased voltage and calcium-dependent activation. Corresponding to the shifts in voltage dependence of activation, the D434G currents activated faster than the wild-type currents in response to a depolarizing voltage pulse (Fig. 4a,c). These results suggest that during an action potential in neurons, in response to depolarization and  $\text{Ca}^{2+}$  entry through voltage-dependent  $\text{Ca}^{2+}$  channels, more mutant BK channels open, causing a rapid repolarization of the action potential<sup>8</sup>.

To define better the mechanism of the increase in macroscopic currents, we made single-channel recordings from BK channels expressed in CHO cells. Both the wild-type channel and the D434G mutant channel were activated by an increase in voltage or in intracellular  $\text{Ca}^{2+}$  concentration, but at a given voltage and  $\text{Ca}^{2+}$  concentration, the mutant channel spent substantially more time in the open state (Fig. 5a). At a given  $\text{Ca}^{2+}$  concentration, the mutant channel was activated at lower voltages (Fig. 5b). There was no difference in the Boltzmann's slope factors for single channels (wild-type,  $9.7 \pm 4.1$  (mean  $\pm$  s.d.),  $n = 9$ ; D434G,  $8.8 \pm 3.7$ ,  $n = 24$ ;  $P > 0.05$ ), and the difference in voltage sensitivity was smaller at saturating levels of  $\text{Ca}^{2+}$ . These data suggest that the primary effect of the mutation was to increase  $\text{Ca}^{2+}$  sensitivity three- to fivefold (Fig. 5c,d), rather than to affect the voltage sensor, which is consistent with the role of the RCK domain as a high-affinity site for  $\text{Ca}^{2+}$  binding. Mutations of the  $\alpha$  subunit are known to decrease  $\text{Ca}^{2+}$  sensitivity of BK channels<sup>9</sup>, but none have been reported to increase  $\text{Ca}^{2+}$  sensitivity. There are other mechanisms by which  $\text{Ca}^{2+}$  sensitivity can be increased, such as by association of the  $\alpha$  subunit with the  $\beta$

subunit<sup>10,11</sup>; a mutation of the  $\beta 1$  subunit (a predominant isoform in smooth muscle) that further increases  $\text{Ca}^{2+}$  sensitivity was recently identified<sup>12</sup>. Consistent with the location of the mutation remote from the pore region, there was no change in single-channel conductance (wild-type,  $185 \pm 16$  pS (mean  $\pm$  s.d.),  $n = 11$ ; D434G,  $180 \pm 20$  pS,  $n = 11$ ;  $P > 0.05$ ). We obtained similar results for single-channel properties from oocyte recordings (data not shown).

An increase in  $\text{Ca}^{2+}$  sensitivity of the BK channel leads to greater macroscopic potassium conductance under physiological conditions. Thus, the D434G mutation leads to a gain of function of the  $\alpha$  subunit. There are several reasons why gain of function of the BK channel could lead to an increase in brain excitability, causing generalized epilepsy when the thalamus or thalamocortical circuits are involved and paroxysmal dyskinesia when the basal ganglia is involved. The most likely mechanism relates to the more rapid repolarization of action potentials by D434G mutant channels. Enhancing this repolarization enables faster repriming (removal of inactivation) of sodium channels and thus allows neurons to fire at a higher frequency<sup>8,13,14</sup>. Alternatively, enhancing some inhibitory currents can switch neurons in a circuit into a bursting mode, as can occur with absence seizures that depend on activation of inhibitory GABA<sub>B</sub> receptors in the thalamus<sup>15</sup>. Likewise, gain of function of BK channels could lead to greater hyperpolarization and activate the hyperpolarization-activated cation current ( $I_h$ )<sup>16</sup>, resulting in generation of secondary depolarizations. Another possible explanation is that if BK channels are present in GABAergic neurons, an increase in inhibition of these neurons could lead to disinhibition of a neuronal network.

Ethanol can directly activate the BK channel *in vivo* in *Caenorhabditis elegans*<sup>17</sup>. This finding may explain the observation that alcohol triggers dyskinesias in certain individuals in the family reported here. The ability of alcohol to trigger PNKD is well recognized, but the detailed mechanism is still under investigation<sup>18</sup>. The gain-of-function mutation D434G may have a synergistic effect with ethanol to trigger the onset of the symptoms.

Knockout mice deficient in the BK channel  $\beta 4$  subunit were recently created and characterized (R. Brenner, personal communication).

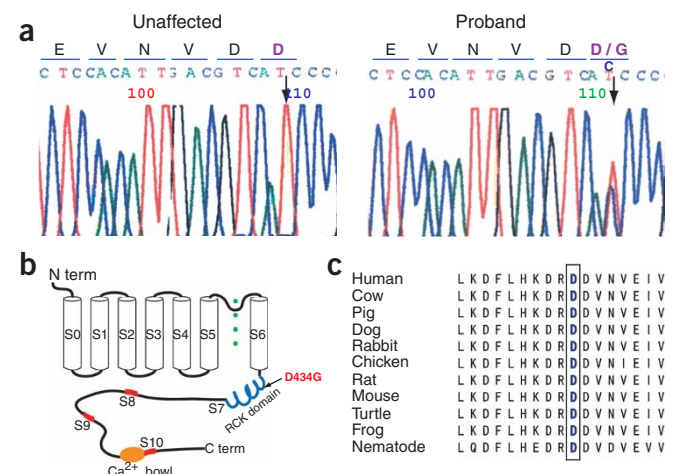


**Figure 3** *KCNMA1* mutation 1301A→G cosegregates with GEPD in kindred QW1378. (a) DNA sequence analysis of exon 10 of *KCNMA1* from an unaffected individual (individual III-10) and the proband (individual IV-8) identified an A→G substitution (reverse sequence) at codon 434 in the proband, which results in the replacement of a negatively charged aspartic acid residue with a neutral amino acid (glycine, D434G). (b) Structure of the BK channel with the D434G mutation indicated. (c) Asp434 of *KCNMA1* is evolutionally conserved among different species.

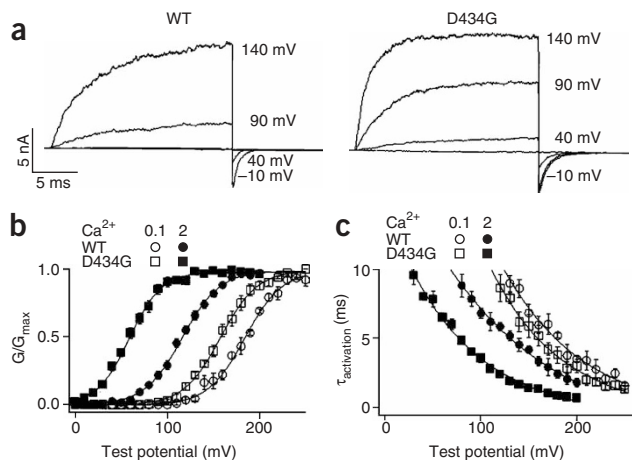


**Figure 4** Electrophysiological characterization of wild-type and D434G mutant KCNMA1 potassium channels in *X. laevis* oocytes. **(a)** Selected current traces of wild-type (WT; left) and D434G mutant (right) channels at  $\text{Ca}^{2+}$  concentration of  $2 \mu\text{M}$ . Test potentials were  $-10$  to  $+140$  mV with  $50$ -mV increments. The holding and repolarizing potentials were  $-80$  and  $-50$  mV, respectively. **(b)** Mean G-V relations of wild-type (WT) and D434G mutant channels at  $\text{Ca}^{2+}$  concentrations of  $0.1$  and  $2 \mu\text{M}$ . All G-V relations are fitted with the Boltzmann relation (solid lines) with  $V_{1/2}$  and slope factor at  $2 \mu\text{M}$  ( $116 \pm 5$  mV,  $20.6 \pm 4.4$  for wild-type and  $58.9 \pm 4.8$  mV,  $17.6 \pm 4.3$  for D434G) and at  $0.1 \mu\text{M}$  ( $184 \pm 8$  mV,  $20.5 \pm 6.3$  for wild-type and  $157 \pm 5$  mV,  $20.3 \pm 4.2$  for D434G). **(c)** Plots of activation time constants of wild-type (WT) and D434G mutant channels as a function of test potential at  $\text{Ca}^{2+}$  concentrations of  $0.1$  and  $2 \mu\text{M}$ . The curves are fitted with an exponential function (solid lines).

The  $\beta 4$  subunit is a neuron-specific inhibitory subunit for the BK current. Mice lacking the BK  $\beta 4$  subunit had a gain of function of BK channels, increased firing rate of knockout cells and spontaneous nonconvulsive seizures (epilepsy). Treatment with paxilline, a specific blocker for BK channels, reduced the firing rate. These results support our conclusion that gain of function of the BK channel causes GEPD.

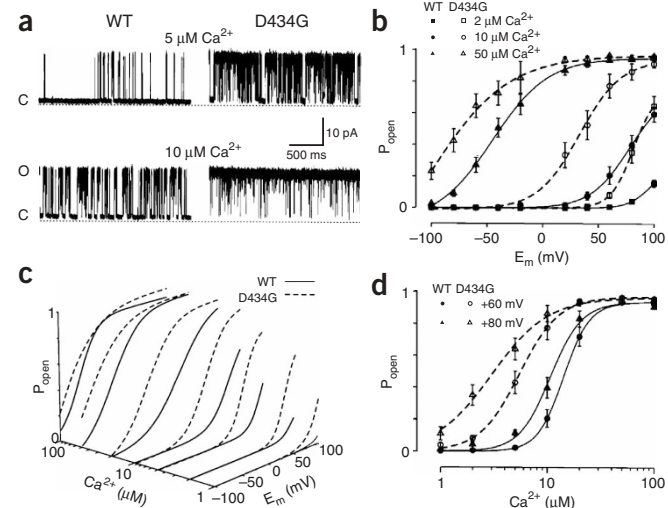
The *in vivo* physiological roles of *KCNMA1* remain intriguing. Mice homozygously deficient in *Kcnma1* have abnormal conditioned eye-blink reflex and abnormal locomotion and motor coordination<sup>19</sup>. These mice also develop high-frequency hearing loss at 8 weeks of age<sup>20</sup>. The phenotype of humans with the *KCNMA1* mutation 1301A→G seems to be very different from that reported for the knockout mice. One major reason for this difference may be that the human missense mutation is a gain-of-function mutation, whereas the mice lacked BK channels.

Our results provide insight into the pathophysiological role of the BK potassium channel in the central nervous system: abnormally increased BK channel activity can cause epilepsy and dyskinesia. Syndromes of coexistent epilepsy and paroxysmal dyskinesia have been reported, including autosomal dominant benign infantile convulsions and paroxysmal choreoathetosis (ICCA)<sup>21</sup> and related syndromes<sup>22</sup>. The ICCA phenotype is characterized by paroxysmal

kinesigenic dyskinesia (PKD) and generalized convulsions in infancy and has been linked to chromosome 16p, but the specific gene underlying the phenotype has not been identified yet<sup>21</sup>. The GEPD phenotype described here differs from ICCA in both the type of seizures and paroxysmal dyskinesia expressed, and linkage to 16p was not observed. PKD has been observed in one affected individual from a family with myokymia and paroxysmal ataxia and a mutation in the potassium channel gene *KCNA1* (ref. 23). Different mutations in *KCNA1* are associated with different neurological phenotypes, including partial seizures<sup>24</sup>, but *KCNA1* mutations have not been reported as a cause of coexistent seizures and paroxysmal dyskinesia in a single individual. Mutations in potassium channel genes *KCNQ2* and *KCNQ3* are associated with benign familial neonatal seizures<sup>4</sup>, which are different from the absence seizures and generalized tonic-clonic seizures reported here. The phenotype reported here most closely resembles a case series of individuals with early-onset absence epilepsy and paroxysmal dyskinesia<sup>3</sup>. The relationship between epilepsy and paroxysmal dyskinesia is complex, and the full spectrum of coexistent syndromes remains to be defined, but the GEPD syndrome described here seems to be distinct from those reported to date.

In summary, this study identifies a new genetic locus for GEPD on chromosome 10q22 and establishes that mutations of the BK channel cause GEPD. Our study also suggests that BK channel-blocking agents might be used as a potential therapy for epilepsy and paroxysmal dyskinesia.

**Figure 5** The D434G mutation of KCNMA1 potassium channels caused an increase in open-channel probability ( $P_{\text{open}}$ ), consistent with an increase in sensitivity to  $\text{Ca}^{2+}$ . **(a)** Single-channel currents recorded from wild-type (WT; left) and D434G mutant KCNMA1 channels (right) expressed in CHO cells. With intracellular free  $\text{Ca}^{2+}$  concentrations of  $5 \mu\text{M}$  (upper traces) and  $10 \mu\text{M}$  (lower traces), the mutant channel was more likely to be in the open state. There was no difference in single-channel conductance. C, closed state; O, open state; dotted lines, zero current level. Membrane potential =  $+80$  mV. **(b)** Effect of membrane potential on  $P_{\text{open}}$  of wild-type and D434G mutant channels at three  $\text{Ca}^{2+}$  concentrations ( $2$ ,  $10$  and  $50 \mu\text{M}$ ). Lines are fit to the Boltzmann equation. **(c)** Relationship between intracellular free  $\text{Ca}^{2+}$  concentration, membrane potential and  $P_{\text{open}}$ . Each line is the Boltzmann fit obtained as in **b**. The difference between curves becomes less at high concentrations of  $\text{Ca}^{2+}$ , consistent with saturation of calcium binding. **(d)** Relationship between  $P_{\text{open}}$  and  $\text{Ca}^{2+}$  concentrations at membrane potentials of  $+60$  mV and  $+80$  mV in wild-type (WT) and D434G mutant channels. Lines are fit to the Hill equation. **(b-d)** Solid lines, wild-type; dashed lines, D434G mutant channels.  $n = 5-17$  patches for each point. Error bars represent s.e.m.





## METHODS

**Human subjects.** This study was approved by the Cleveland Clinic Institutional Review Board on Human Subjects. Informed consent was obtained from all participants or their guardians. The affected individuals and family members were identified and clinically characterized at the Department of Neurology of the Cleveland Clinic Foundation. The family under study is of mixed European descent and was referred to this study from the adult epilepsy clinic as a result of the diagnosis of epilepsy in multiple family members. We constructed a detailed pedigree. We obtained clinical information through semistructured interviews in person and by telephone, carried out by a neurologist with specialty training in epilepsy and clinical neurophysiology. Seizure histories were corroborated by eyewitnesses when possible. When applicable, we obtained records of interictal EEG and video-EEG. We defined epilepsy as two or more unprovoked seizures. We classified seizure types in accordance with the International Classification of Epileptic Seizures<sup>25</sup>. We classified epilepsy syndromes in accordance with the International Classification of Epilepsies and Epileptic Syndromes<sup>26</sup>.

The proband (individual IV-8; **Fig. 1a**) was 21 years old when she was interviewed. She had normal birth and early development. Routine neurological exam gave normal results. At 2 years of age, she developed episodes of involuntary mouth movement and hand stiffness, lasting 10 s to 2 min, with preserved consciousness; these occurred weekly, were more common with fatigue, were not triggered by sudden movement and were diagnosed as paroxysmal dyskinesia. At approximately the same age, she developed separate episodes of loss of awareness, with vacant staring and unresponsiveness, characteristic of typical absence seizures. There was no aura, and these absence seizures occurred daily in early childhood, progressively decreasing in frequency to monthly seizures in adolescence, with medication. Routine EEG showed generalized spike-wave complexes.

Her paternal first cousin (individual IV-1) had episodes of vacant staring and episodes of paroxysmal dyskinesia without loss of awareness. She was evaluated with inpatient continuous video-EEG. Her interictal EEG showed generalized spike-wave complexes. Episodes of vacant staring and eyelid fluttering were associated with bursts of generalized spike-wave complexes, confirming their epileptic nature. Episodes of paroxysmal dyskinesia were not associated with any EEG change, confirming their nonepileptic nature. At 5 years of age, she developed generalized tonic-clonic seizures.

Epileptic seizures, in other family members affected with epilepsy, were typically absence seizures, with generalized tonic-clonic seizures in two other individuals (individuals IV-1 and IV-2). The age of onset of absence seizures in the family is earlier than usual for typical absence seizures, but such an early age of onset has been described in a series of individuals with coexistent absence epilepsy and paroxysmal dyskinesia<sup>3</sup>. The seizure types exhibited by this family have no resemblance to benign familial neonatal seizures or benign infantile convulsions. There was no evidence for myoclonic seizures in any of the affected individuals.

The proband's seizures were responsive to valproate and lamotrigine. The seizure frequency in the proband has varied from daily (when she was younger and not taking medications regularly) to monthly (her seizure frequency in current years on valproate and/or lamotrigine). Individuals IV-1 and IV-2 had seizures and paroxysmal dyskinesia partially responsive to clonazepam.

Paroxysmal dyskinesia can be broadly classified into two main subtypes: PKD, if the attacks are induced by sudden movement, and PNKD, if they are not<sup>18,27</sup>. Paroxysmal dyskinesias, in those affected, were often described as involuntary dystonic or choreiform movements of the mouth, tongue and extremities, nonkinesigenic but induced by alcohol, fatigue and stress, most consistent with PNKD. PNKD in this family had onset in childhood and showed a gradual decrease in frequency with age but persisted into the fourth decade in some individuals. The human subjects had no complaints of hearing loss or other neurological symptoms and had no evidence for hearing loss on routine neurological exam.

**Genotyping and linkage analysis.** We prepared human genomic DNA from whole blood with the DNA Isolation Kit for Mammalian Blood (Roche Diagnostic Co). We carried out genome-wide genotyping using 382 polymorphic, fluorescently labeled microsatellite markers on chromosomes 1–22 (ABI PRISM Linkage Mapping Set-MD10) as described previously<sup>28</sup>. We

identified additional markers in the Genethon database and used them for fine mapping and haplotype analysis. We genotyped markers using an ABI 3100 Genetic Analyzer (Applied Biosystems). Allele-calling was carried out by GeneScan and GeneMapper 2 software programs (Applied Biosystems). We carried out linkage analysis and calculated two-point lod scores using the Linkage Package 5.2, assuming autosomal dominant inheritance, penetrance of 99%, a phenocopy rate of 0%, gene frequency of 1/10,000 and allele frequency of 1/*n* (where *n* equals the number of alleles observed).

**Mutational analysis.** We carried out mutation analysis using direct DNA sequence analysis. We determined the genomic structure of *KCNMA1* by comparing its 3,537-bp cDNA sequence to its genomic sequence and found that it contained 27 exons. We then designed PCR primers (sequences available on request) based on intronic sequences to amplify all 27 coding exons. We purified PCR products from agarose gels using the QIAquick PCR Purification Kit (QIAGEN) and sequenced them with both forward and reverse primers using an ABI3100 Genetic Analyzer (Applied Biosystems). We used restriction fragment length polymorphism analysis to confirm the D434G mutation and to test the presence or absence of the mutation in other family members and 400 normal controls. The D434G mutation creates a *Tsp45I* restriction site. We digested the 201-bp PCR fragment containing exon 10, where the 1301A → G mutation is located, by incubating it with *Tsp45I*. We separated the digested product on 2% agarose gels and analyzed it.

**Cloning and mutagenesis.** We cloned human *KCNMA1* cDNA into plasmid pcDNA3, resulting in an expression construct for the BK channel (gifts from I.B. Levitan and Y. Zhou, University of Pennsylvania School of Medicine, and from L. Salkoff and A. Butler, Washington University Medical School). We introduced the D434G mutation into the *KCNMA1-pcDNA3* construct using PCR-based site-directed mutagenesis and confirmed it by sequencing the full *KCNMA1* insert. To create the expression constructs for *X. laevis* oocyte expression, we subcloned the full-length wild-type and mutated *KCNMA1* cDNAs into the pSP64 Poly(A) vector (*KCNMA1-pSP64*) using restriction enzymes *HindIII* and *XbaI*.

**Electrophysiological characterization of human BK channels in *X. laevis* oocytes.** We digested *KCNMA1-pSP64* DNA with *EcoRI* and prepared cRNA using the *In Vitro* Transcription kit with SP6 polymerase. We injected 5 ng of cRNA into each *X. laevis* oocyte 2–6 d before recording. We recorded macroscopic currents from inside-out patches formed with borosilicate pipettes of 0.9–1.8 MΩ resistance. We acquired data using an Axopatch 200-B patch clamp amplifier (Axon Instruments) and Pulse acquisition software (HEKA Elektronik). We digitized records at 20-μs intervals and low pass-filtered them at 10 kHz with the Axopatch's 4 pole Bessel filter. During G-V measurements, the series resistance at maximum current amplitude will typically cause a voltage error ≤ 5 mV. The error will be smaller at voltages at which the activation of channels is not saturated. The shape of the G-V relation and its voltage range affected by this error are smaller than the standard deviation (**Fig. 4**). The pipette solution contained 140 mM K-methanesulfonic acid, 20 mM HEPES buffer, 2 mM KCl and 2 mM MgCl<sub>2</sub> (pH 7.20). The basal internal solution contained 140 mM K-methanesulfonic acid, 20 mM HEPES buffer, 2 mM KCl and 1 mM EGTA (pH 7.20). We added CaCl<sub>2</sub> to internal solutions to give the appropriate free intracellular Ca<sup>2+</sup> concentration. All recordings were obtained at room temperature (22–24 °C).

**Electrophysiological characterization of human BK channels in mammalian cells.** For single-channel recordings from CHO cells, we subcloned *KCNMA1* cDNA (wild-type and mutated) into a pIRES2-EGFP vector (Clontech) with the restriction enzymes *NheI* and *XhoI*. We plated CHO cells onto coverslips in 12-well Falcon plates and transfected them with 0.8 μg of DNA per well using lipofectamine (4 μl per well; Life Technologies) 6–12 h before recording. We placed coverslips in a recording chamber on an inverted light microscope (Axiocvert 100, Zeiss) and superfused them with Ringer solution at 2 ml min<sup>-1</sup>. We selected transfected cells by visualizing GFP fluorescence. We made patch-clamp recordings with borosilicate glass electrodes fabricated using a P-97 microelectrode puller (Sutter Instruments). We filled microelectrodes (20–100 MΩ) with a solution containing 144 mM KCl, 16 mM NaCl, 2 mM MgCl<sub>2</sub>, 2 mM TES, 11 mM glucose, 0.065 mM CaCl<sub>2</sub> and 0.08 mM EGTA.

After obtaining a patch, we moved the electrode tip into a separate mini-chamber<sup>29</sup> and exposed the inside face of the patch to the same solution (at a flow rate of 1 ml min<sup>-1</sup>) in which we varied the amount of CaCl<sub>2</sub> to give a free Ca<sup>2+</sup> concentration of 1, 2, 5, 10, 20, 50 or 100 μM (calculated using Webmaxc). We recorded single-channel currents in the inside-out configuration from patches with one to six channels at room temperature in voltage clamps from a holding potential of -60 mV to test potentials from -100 to +100 mV (steps of 20 mV for 3 seconds each). We low pass-filtered the currents at 2 kHz and digitized them at a rate of 10 kHz using an Axopatch 1D amplifier, Digidata 1322a A/D converter and PClamp software (Axon Instruments). We determined the number of channels in each patch using all-points histograms from recordings made at each level of Ca<sup>2+</sup> concentration and voltage. If these histograms did not indicate the number of channels present, then we rejected the data from that patch. We analyzed the open-channel probability using Clampfit software (Axon Instruments) and fit the data to the Boltzmann and Hill equations using Origin Software (OriginLab Corp).

**URL.** Webmaxc is available at <http://www.stanford.edu/~cpatton/maxc.html>.

**GenBank accession number.** *KCNMA1* cDNA sequence, NM\_002247.

*Note: Supplementary information is available on the Nature Genetics website.*

#### ACKNOWLEDGMENTS

We thank I.B. Levitan, Y. Zhou, L. Salkoff and A. Butler for the expression constructs for *KCNMA1*; the study participants for their enthusiasm for and support of this study; L. Li for lod score calculation; S. Yong, G. Kirsch, C.J. Lingle, T. Zhang, A. Alexopoulos and I. Najm for help and discussion; and R. Guerrini for providing DNA from two individuals with epilepsy and paroxysmal dyskinesia<sup>3</sup> (no *KCNMA1* mutation was identified in these two DNA samples). This work was supported by grants from the US National Institutes of Health (Q.K.W., J.F.B., G.B.R. & A.D.-S. and J.C.), an American Heart Association Established Investigator award (Q.K.W.), the VAMC (G.B.R.) and a Clinical Research Training Fellowship from the American Academy of Neurology Foundation (J.F.B.). This work was supported in part by the Chinese Ministry of Science and Technology National High Technology 863 Project grant (Q.K.W.) and a Public Health Service National Center for Research Resources grant at the Cleveland Clinic Foundation (Q.K.W.).

#### COMPETING INTERESTS STATEMENT

The authors declare that they have no competing financial interests.

Received 4 February; accepted 5 May 2005

Published online at <http://www.nature.com/naturegenetics/>

1. World Health Organization. World Health Report 2002. (World Health Organization, Geneva, Switzerland, 2002).
2. Guerrini, R. Idiopathic epilepsy and paroxysmal dyskinesia. *Epilepsia* **42**, 36–41 (2001).
3. Guerrini, R. *et al.* Early-onset absence epilepsy and paroxysmal dyskinesia. *Epilepsia* **43**, 1224–1229 (2002).
4. Noebels, J.L. The biology of epilepsy genes. *Annu. Rev. Neurosci.* **26**, 599–625 (2003).
5. Browne, D.L. *et al.* Episodic ataxia/myokymia syndrome is associated with point mutations in the human potassium channel gene, *KCNA1*. *Nat. Genet.* **8**, 136–140 (1994).

6. Shi, J. *et al.* Mechanism of magnesium activation of calcium-activated potassium channels. *Nature* **418**, 876–880 (2002).
7. Xia, X.M., Zeng, X. & Lingle, C.J. Multiple regulatory sites in large-conductance calcium-activated potassium channels. *Nature* **418**, 880–884 (2002).
8. Adams, P.R., Constanti, A., Brown, D.A. & Clark, R.B. Intracellular Ca<sup>2+</sup> activates a fast voltage-sensitive K<sup>+</sup> current in vertebrate sympathetic neurones. *Nature* **296**, 746–749 (1982).
9. Bao, L., Rapin, A.M., Holmstrand, E.C. & Cox, D.H. Elimination of the BK(Ca) channel's high-affinity Ca<sup>2+</sup> sensitivity. *J. Gen. Physiol.* **120**, 173–189 (2002).
10. McManus, O.B. *et al.* Functional role of the beta subunit of high conductance calcium-activated potassium channels. *Neuron* **14**, 645–650 (1995).
11. Nimigeon, C.M. & Magleby, K.L. The beta subunit increases the Ca<sup>2+</sup> sensitivity of large conductance Ca<sup>2+</sup>-activated potassium channels by retaining the gating in the bursting states. *J. Gen. Physiol.* **113**, 425–440 (1999).
12. Fernandez-Fernandez, J.M. *et al.* Gain-of-function mutation in the KCNB1 potassium channel subunit is associated with low prevalence of diastolic hypertension. *J. Clin. Invest.* **113**, 1032–1039 (2004).
13. Jin, W., Sugaya, A., Tsuda, T., Ohguchi, H. & Sugaya, E. Relationship between large conductance calcium-activated potassium channel and bursting activity. *Brain Res.* **860**, 21–28 (2000).
14. Lancaster, B. & Nicoll, R.A. Properties of two calcium-activated hyperpolarizations in rat hippocampal neurones. *J. Physiol. (Lond.)* **389**, 187–203 (1987).
15. von Krosigk, M., Bal, T. & McCormick, D.A. Cellular mechanisms of a synchronized oscillation in the thalamus. *Science* **261**, 361–364 (1993).
16. McCormick, D.A. & Pape, H.C. Properties of a hyperpolarization-activated cation current and its role in rhythmic oscillation in thalamic relay neurones. *J. Physiol. (Lond.)* **431**, 291–318 (1990).
17. Davies, A.G. *et al.* A central role of the BK potassium channel in behavioral responses to ethanol in *C. elegans*. *Cell* **115**, 655–666 (2003).
18. Lee, H.Y. *et al.* The gene for paroxysmal non-kinesigenic dyskinesia encodes an enzyme in a stress response pathway. *Hum. Mol. Genet.* **13**, 3161–3170 (2004).
19. Sausbier, M. *et al.* Cerebellar ataxia and Purkinje cell dysfunction caused by Ca<sup>2+</sup>-activated K<sup>+</sup> channel deficiency. *Proc. Natl. Acad. Sci. USA* **101**, 9474–9478 (2004).
20. Rüttiger, L. *et al.* Deletion of the Ca<sup>2+</sup>-activated potassium (BK) alpha-subunit but not the BKbeta1-subunit leads to progressive hearing loss. *Proc. Natl. Acad. Sci. USA* **101**, 12922–12927 (2004).
21. Szepeetowski, P. *et al.* Familial infantile convulsions and paroxysmal choreoathetosis: a new neurological syndrome linked to the pericentromeric region of human chromosome 16. *Am. J. Hum. Genet.* **61**, 889–898 (1997).
22. Guerrini, R. *et al.* Autosomal recessive rolandic epilepsy with paroxysmal exercise-induced dystonia and writer's cramp: delineation of the syndrome and gene mapping to chromosome 16p12–112. *Ann. Neurol.* **45**, 344–352 (1999).
23. Lubbers, W.J. *et al.* Hereditary myokymia and paroxysmal ataxia linked to chromosome 12 is responsive to acetazolamide. *J. Neurol. Neurosurg. Psychiatry* **59**, 400–405 (1995).
24. Eunson, L.H. *et al.* Clinical, genetic, and expression studies of mutations in the potassium channel gene *KCNA1* reveal new phenotypic variability. *Ann. Neurol.* **48**, 647–656 (2000).
25. Commission on Classification and Terminology of the International League Against Epilepsy. Proposal for revised clinical and electroencephalographic classification of epileptic seizures. *Epilepsia* **22**, 489–501 (1981).
26. Commission on Classification and Terminology of the International League Against Epilepsy. Proposal for revised classification of epilepsies and epileptic syndromes. *Epilepsia* **30**, 389–399 (1989).
27. Demirkiran, M. & Jankovic, J. Paroxysmal dyskinesias: clinical features and classification. *Ann. Neurol.* **38**, 571–579 (1995).
28. Wang, L., Fan, C., Topol, S.E., Topol, E.J. & Wang, Q. Mutation of MEF2A in an inherited disorder with features of coronary artery disease. *Science* **302**, 1578–1581 (2003).
29. Barrett, J.N., Magleby, K.L. & Pallotta, B.S. Properties of single calcium-activated potassium channels in cultured rat muscle. *J. Physiol. (Lond.)* **331**, 211–230 (1982).